

Pair transfer and the sub-barrier fusion of $^{18}\text{O} + ^{58}\text{Ni}$

A. M. Borges

Departamento de Física, Universidade Federal Fluminense, Niterói, 2420, Rio de Janeiro, Brazil

C. P. da Silva, D. Pereira, L. C. Chamon, and E. S. Rossi, Jr.

Instituto de Física, Universidade de São Paulo, Caixa Postal 20516, São Paulo, 01498, São Paulo, Brazil

C. E. Aguiar

Instituto de Física, Universidade Federal do Rio de Janeiro, Caixa Postal 68528, Rio de Janeiro, 21945, Rio de Janeiro, Brazil

(Received 14 April 1992)

Evaporation residue cross sections for the $^{18}\text{O} + ^{58}\text{Ni}$ and $^{16}\text{O} + ^{60}\text{Ni}$ fusion reactions have been measured in the energy range from 3 below to 20 MeV above the Coulomb barrier. The low-energy fusion enhancements found in the two systems are very different. A comparative analysis suggests that collective pair transfer modes play an important role in the sub-barrier fusion of $^{18}\text{O} + ^{58}\text{Ni}$.

PACS number(s): 25.70.Jj

The mechanisms by which heavy ions fuse at energies below the Coulomb barrier are not yet understood in detail. Many different ideas have been proposed to explain the enhancement of measured sub-barrier fusion cross sections with respect to the predictions of one-dimensional barrier penetration models [1-3]. This enhancement has been related to the effects of low-energy surface vibrations [4], static deformations [5], coupling to reaction channels [6], neck formation [7], and neutron flow [8].

In particular, several attempts have been made to isolate the role of transfer channels with positive Q values [9-11], which are expected to produce some very characteristic structures in the low-energy fusion excitation functions [6]. A projectile-target combination that looks interesting for this kind of study is $^{18}\text{O} + ^{58}\text{Ni}$, as in this system the two-neutron stripping channel has a very large ground-state Q value, $Q = 8.2$ MeV, amounting to almost 25% of the Coulomb barrier height.

In this paper we report upon measurements of the evaporation residue cross sections for the system $^{18}\text{O} + ^{58}\text{Ni}$ in the energy range $30 < E_{c.m.} < 50$ MeV. In order to set apart more clearly the neutron transfer effects from those generated by the inelastic channels we also measured the $^{16}\text{O} + ^{60}\text{Ni}$ excitation function in a similar energy range.

The $^{16,18}\text{O}$ beams were provided by the University of São Paulo 8UD Pelletron Accelerator. The nickel targets were self-supported ($\approx 40 \mu\text{g}/\text{cm}^2$) and isotopically enriched ($\approx 99\%$). A surface barrier counter serving as a beam intensity monitor has been mounted at $\theta_{lab} = 26.8^\circ$. Evaporation residue cross section were measured using the time-of-flight technique in connection with an electrostatic deflector which removed most of the beamlike flux. The evaporation residues were implanted behind the deflector into a surface barrier detector and the time of flight was measured against the signal of a plastic scintillator downstream from the target. This array gives rise to a flight distance of 76 cm. In order to reduce background due to scattering on slits and collimators, these

were removed and a powerful control method for the on-target beam flux was employed [12]. The time resolution was about 1 ns, and the energy resolution was up to 2.5%. A typical time-of-flight vs energy spectrum is shown in Fig. 1. The mass resolution is approximately $\Delta A/A = \frac{1}{60}$. The angular distributions for the evaporation residues have been measured in the interval $3^\circ < \theta_{lab} < 18^\circ$. Two of these angular distributions are shown in Fig. 2. This experimental setup has already been used to measure fusion cross sections for other systems in the same mass region [13,14].

The measured fusion cross sections for $^{18}\text{O} + ^{58}\text{Ni}$ and $^{16}\text{O} + ^{60}\text{Ni}$ are given in Table I and displayed in Fig. 3.

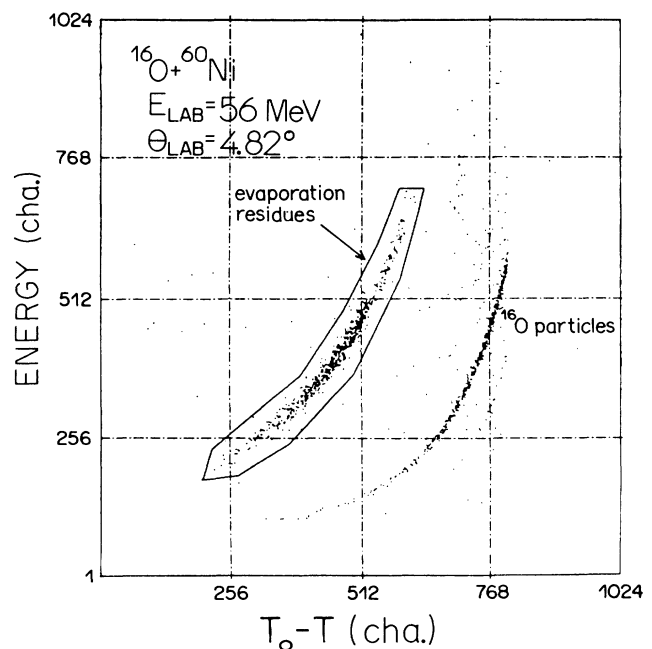


FIG. 1. Typical time-of-flight vs energy spectrum for the $^{16}\text{O} + ^{60}\text{Ni}$ system.

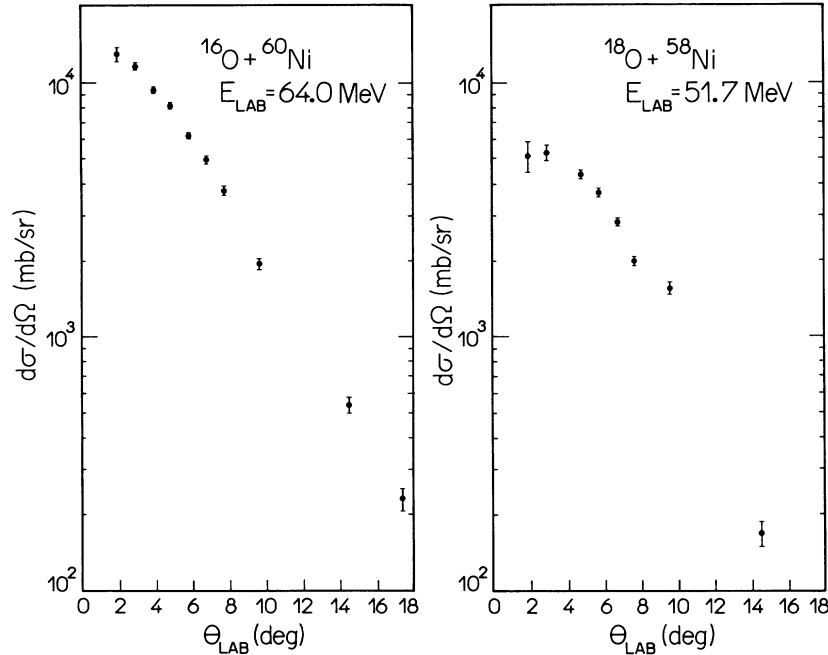


FIG. 2. Angular distributions of evaporation residues for the $^{16}\text{O}+^{60}\text{Ni}$ reaction at $E_{\text{lab}}=64.0$ MeV (left), and $^{18}\text{O}+^{58}\text{Ni}$ at $E_{\text{lab}}=51.7$ MeV (right).

The dashed lines in this figure represent calculations carried out with a one-dimensional barrier penetration model. In these calculations we have used the Krappé-Nix-Sierk potential [15], and for each system the radius parameter r_0 was adjusted to obtain the best fit of data in the interval $200 < \sigma_{\text{fus}} < 600$ mb. We found $r_0=1.11$ fm for the $^{18}\text{O}+^{58}\text{Ni}$ system and $r_0=1.09$ fm for $^{16}\text{O}+^{60}\text{Ni}$. The corresponding values for the Coulomb barrier height V_B and radius R_B are given in Table II. We observe from Fig. 3 that at energies below the Coulomb barrier the

fusion cross sections are much larger than the one-dimensional predictions.

One way of explaining this enhancement is to consider the zero-point motion of the nuclear surface associated to

TABLE I. Measured fusion cross sections for the systems investigated in this work.

System	$E_{\text{c.m.}}$ (MeV)	σ_{fus} (mb)	$\Delta\sigma_{\text{fus}}$ (mb)	System	$E_{\text{c.m.}}$ (MeV)	σ_{fus} (mb)	$\Delta\sigma_{\text{fus}}$ (mb)
$^{18}\text{O}+^{58}\text{Ni}$	29.8	28	4	$^{16}\text{O}+^{60}\text{Ni}$	31.6	23	3
	30.5	41	6		32.4	44	4
	30.9	59	6		33.2	70	8
	31.2	55	5		33.9	98	5
	31.7	64	10		34.7	91	6
	32.3	78	7		36.3	149	7
	32.7	103	7		37.1	233	16
	32.9	139	7		37.9	255	14
	33.2	136	12		38.7	284	16
	34.3	172	7		39.5	335	10
	34.7	178	15		40.3	332	16
	35.5	241	11		41.0	422	17
	36.2	219	15		41.8	458	20
	37.0	294	11		42.6	555	22
	37.9	335	18		43.4	531	20
	39.5	354	14		44.2	531	19
	40.9	496	21		47.4	668	24
42.8	535	23	50.5	667	23		
48.8	789	47	56.8	619	70		

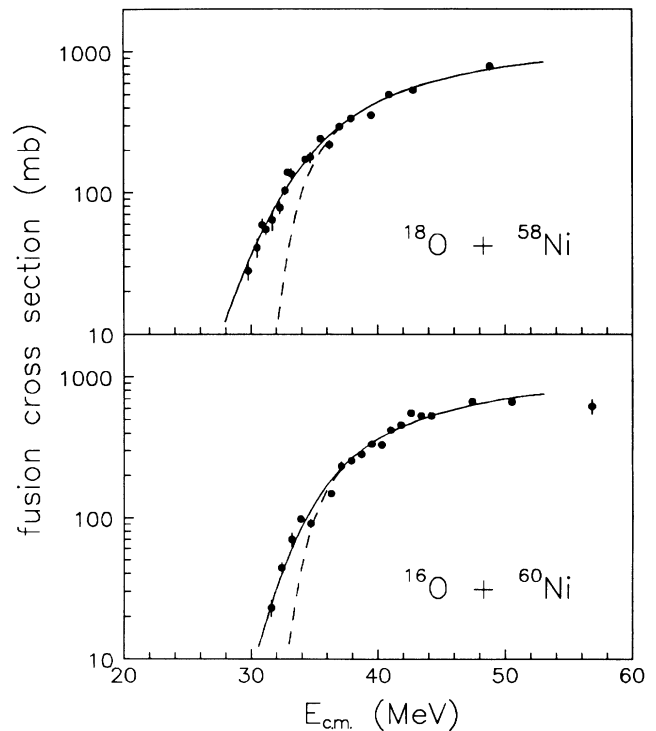


FIG. 3. Fusion cross sections for the $^{18}\text{O}+^{58}\text{Ni}$ and $^{16}\text{O}+^{60}\text{Ni}$ systems. Predictions of the one-dimensional barrier penetration model are indicated by dashed lines. Fits to the experimental data assuming a Gaussian distribution of nuclear radii are shown as full lines.

TABLE II. Fusion barrier parameters obtained from the measured cross sections. V_B and R_B are the height and radius of the Coulomb barrier, and S_R is the standard deviation of fluctuations of the nuclear radii.

System	V_B (MeV)	R_B (fm)	S_R (fm)
$^{18}\text{O}+^{58}\text{Ni}$	32.7	8.96	0.63
$^{16}\text{O}+^{60}\text{Ni}$	33.6	8.70	0.42

low-lying collective vibrations [4]. These quantum fluctuations lead to a random Gaussian distribution of the radii of the colliding nuclei, which will generate corresponding distributions of V_B and R_B . The widths of these latter distributions are proportional to the standard deviation S_R in the sum of projectile and target radii. We calculated the fusion cross section as a folding of the one-dimensional result with the barrier distribution, and obtained the parameter S_R by fitting this average cross section to the experimental data in the range $10 < \sigma_{\text{fus}} < 200$ mb. The best-fit curves are shown as full lines in Fig. 3. The resulting values for S_R , which we take as a measure of the enhancement in each system, are presented in Table II. We note that the $^{18}\text{O}+^{58}\text{Ni}$ system has a more pronounced enhancement than $^{16}\text{O}+^{60}\text{Ni}$, i.e., requires larger fluctuations. The difference (taken in quadrature) between the radius widths of the two systems is

$$\begin{aligned} \Delta S_R &= [S_R(^{18}\text{O}+^{58}\text{Ni})^2 - S_R(^{16}\text{O}+^{60}\text{Ni})^2]^{1/2} \\ &= 0.47 \text{ fm} . \end{aligned}$$

The main purpose of the present work is to understand why the fusion enhancement of $^{18}\text{O}+^{58}\text{Ni}$ is so much larger than that of $^{16}\text{O}+^{60}\text{Ni}$. The low-lying surface vibrations of ^{58}Ni and ^{60}Ni cannot be held responsible for this difference, as they have very similar frequencies and amplitudes. On the other hand, ^{18}O and ^{16}O do show quite different quadrupole modes. The energy of the first 2^+ state of ^{18}O is 2 MeV, which is much lower than the 7 MeV of the corresponding state in ^{16}O . Due to this high energy the quadrupole vibration of ^{16}O should not contribute appreciably to the fusion enhancement, while the frequency of the ^{18}O oscillation is low enough for it to influence considerably the fusion rates. The standard deviation of the radius fluctuation associated to the quadrupole mode is given by

$$S_2 = \frac{R_0}{\sqrt{4\pi}} \beta_2 , \quad (1)$$

where β_2 is the quadrupole deformation parameter and R_0 is the mean nuclear radius. From the experimental result [16] $\beta_2(^{18}\text{O})=0.36$ we find the contribution of the quadrupole mode to the fluctuation of the ^{18}O radius to be $S_2(^{18}\text{O})=0.32\text{fm}$. This value falls short of the observed difference ΔS_R by

$$\delta S_R = [\Delta S_R^2 - S_2(^{18}\text{O})^2]^{1/2} = 0.34 \text{ fm} .$$

The remaining discrepancy δS_R is not explained by any differences in the surface vibrational spectra of the ^{18}O and ^{16}O nuclei.

A possible mechanism for explaining the residual enhancement δS_R lies in another kind of collective mode: pairing vibrations. These oscillations are related to two-nucleon transfer channels, which are very different in the $^{18}\text{O}+^{58}\text{Ni}$ and $^{16}\text{O}+^{60}\text{Ni}$ systems. In the former, as we have mentioned, the $2n$ -stripping reaction has an extremely large ground-state Q value, while no transfer channel with $Q > 0$ is found in the second system. The inclusion of these pair transfer modes in our discussion of the fusion enhancement is greatly simplified if we make use of a macroscopic model in which the gauge-space pairing vibrations are related to displacements of the nuclear surface [17–19]. In this model the pairing deformation parameter β_p is connected to the standard deviation S_p of fluctuation of the nuclear radius by

$$S_p = \sqrt{2} \frac{R_0}{3A_0} \beta_p , \quad (2)$$

where R_0 and A_0 are the mean radius and mass number of the nucleus, and the $\sqrt{2}$ factor accounts for the superposition of pair addition and removal modes, assumed to have equal amplitudes. We consider only the pairing vibrations of the nickel nuclei, as they have a low excitation energy (3 MeV). The oxygen pairing modes are much more stiff, and are thus disregarded. Moreover, because of the large ground-state Q value for two-neutron stripping in the $^{18}\text{O}+^{58}\text{Ni}$ system, we may consider the oxygen nucleus as a good reservoir of neutron pairs that can be used to excite the nickel pairing vibration. This does not happen in the $^{16}\text{O}+^{60}\text{Ni}$ case and the nickel pairing mode should not influence the fusion of this system, as the neutron pairs necessary to excite the vibration are not easily available. From this point of view we can understand the origin of the residual enhancement difference δS_R : it should correspond to the nickel pairing vibration excited in the $^{18}\text{O}+^{58}\text{Ni}$ reaction. Taking $\delta S_R = S_p(^{58}\text{Ni})$ gives $\beta_p = 9.0$ for the pairing deformation parameter. This value is very close to the result $\beta_p = 9.7$ obtained from analysis of the $^{64}\text{Ni}(^{18}\text{O},^{16}\text{O})^{66}\text{Ni}$ transfer reaction [17]. It also agrees with the BCS estimate [19] $\beta_p = 2\Delta/G$, which for a gap parameter $\Delta = 1.6$ MeV and pairing strength [20] $G = 0.33$ MeV again leads to $\beta_p = 9.7$.

In summary, we have found evidence that two-neutron transfer reactions contribute markedly to the sub-barrier fusion of $^{18}\text{O}+^{58}\text{Ni}$. A simple model based on the effects of zero-point pairing fluctuations seems to account very well for the measured enhancement.

We would like to thank R. Pengo for valuable suggestions. This work has been partially supported by CNPq, FAPESP, and FINEP.

- [1] M. Beckerman, *Phys. Rep.* **129**, 145 (1985).
- [2] *Fusion Reactions Below the Coulomb Barrier*, edited by S. G. Steadman, *Lecture Notes in Physics*, Vol. 219 (Springer-Verlag, Berlin, 1985).
- [3] *Heavy Ion Interactions Around the Coulomb Barrier*, edited by C. Signorini, S. Skorka, P. Spalatore, and A. Vitturi, *Lecture Notes in Physics* Vol. 317 (Springer-Verlag, Berlin, 1988).
- [4] H. Esbensen, *Nucl. Phys.* **A352**, 147 (1981).
- [5] R. G. Stokstad and E. E. Gross, *Phys. Rev. C* **23**, 281 (1981).
- [6] C. H. Dasso, S. Landowne, and A. Winther, *Nucl. Phys.* **A405**, 381 (1983); **A407**, 221 (1983).
- [7] C. E. Aguiar, V. C. Barbosa, L. F. Canto, and R. Donangelo, *Phys. Lett. B* **201**, 22 (1988).
- [8] P. H. Stelson, *Phys. Lett. B* **205**, 190 (1988).
- [9] R. A. Broglia, C. H. Dasso, and S. Landowne, *Phys. Rev. C* **32**, 1426 (1985).
- [10] P. Jacobs, Z. Fraenkel, G. Mamane, and I. Tserruya, *Phys. Lett. B* **175**, 271 (1986).
- [11] A. Menchaca-Rocha, E. Belmont-Moreno, M. E. Brandan, A. Martínez, D. Abriola, M. Elgue, A. Etchegoyen, M. C. Etchegoyen, J. O. Fernandez-Niello, D. E. DiGregorio, M. di Tada, A. O. Machiavelli, A. J. Pacheco, and J. E. Testoni, *Phys. Rev. C* **41**, 2654 (1990).
- [12] D. Pereira, O. Sala, and U. Schnitter, *Nucl. Instrum. Methods A* **267**, 41 (1988).
- [13] D. Pereira, G. R. Razeto, O. Sala, L. C. Chamon, C. A. Rocha, J. C. Acquadro, and C. Tenreiro, *Phys. Lett. B* **220**, 347 (1989).
- [14] L. C. Chamon, D. Pereira, E. S. Rossi, C. P. Silva, G. R. Razeto, A. M. Borges, L. C. Gomes, and O. Sala, *Phys. Lett. B* **275**, 29 (1992).
- [15] H. J. Krappe, J. R. Nix, and A. J. Sierk, *Phys. Rev. C* **20**, 992 (1979).
- [16] S. Raman, C. H. Malarkey, W. T. Milner, C. W. Nestor, Jr., and P. H. Stelson, *At. Data Nucl. Data Tables* **36**, 1 (1987).
- [17] C. H. Dasso and G. Pollarolo, *Phys. Lett.* **155B**, 223 (1985).
- [18] C. H. Dasso and A. Vitturi, *Phys. Rev. Lett.* **59**, 634 (1987).
- [19] D. Bès, P. Lotti, E. Maglione, and A. Vitturi, *Phys. Lett.* **169B**, 5 (1986).
- [20] A. K. Kerman, R. D. Lawson, and M. H. MacFarlane, *Phys. Rev.* **124**, 162 (1961).